Biochimica et Biophysica Acta 1834 (2013) 2712–2721

Contents lists available at ScienceDirect

Biochimica et Biophysica Acta

journal homepage: www.elsevier.com/locate/bbapap

The human topoisomerase 1B Arg634Ala mutation results in camptothecin resistance and loss of inter-domain motion correlation

Ilda D'Annessa [a,1], Cinzia Tesauro [a,1], Zhenxing Wang [a,1], Barbara Arnò [a], Laura Zuccaro [a], Paola Fiorani [b], Alessandro Desideri [a,*]

[a] Department of Biology and Interuniversity Consortium, National Institute Biostructure and Biosystem (INBB), University of Rome Tor Vergata, Via Della Ricerca Scientifica, Rome 00133, Italy
[b] Institute of Translational Pharmacology, National Research Council, CNR, Via Del Fosso del Cavaliere 100, Rome 00133, Italy

ARTICLE INFO

Article history:
Received 11 July 2013
Received in revised form 23 September 2013
Accepted 25 September 2013
Available online 2 October 2013

Keywords:
Linker domain
Camptothecin
Topoisomerase
Molecular dynamics
Single mutation

ABSTRACT

Human topoisomerase 1B, the unique target of the natural anticancer compound camptothecin, catalyzes the unwinding of supercoiled DNA by introducing transient single strand nicks and providing covalent protein–DNA adducts. The functional properties and the drug reactivity of the single Arg634Ala mutant have been investigated in comparison to the wild type enzyme. The mutant is characterized by an identical relaxation and cleavage rate but it displays resistance to camptothecin as indicated by a viability assay of the yeast cells transformed with the mutated protein. The mutant also displays a very fast religation rate that is only partially reduced by the presence of the drug, suggesting that this is the main reason for its resistance. A comparative analysis of the structural–dynamical properties of the native and mutant proteins by molecular dynamics simulation indicates that mutation of Arg634 brings to a loss of motion correlation between the different domains and in particular between the linker and the C-terminal domain, containing the catalytic tyrosine residue. These results indicate that the loss of motion correlation and the drug resistance are two strongly correlated events.

1. Introduction

Human topoisomerase 1B (hTop1B) is a monomeric 765 residue enzyme whose role is to maintain the topological state of DNA during the progression of cellular processes such as transcription and duplication [1–3]. The enzyme relaxes positive and negative supercoils by creating a nick on one strand of the DNA duplex and forming a transient phospho-tyrosine bond. The catalytic cycle is composed by five steps: 1) DNA binding and formation of a non-covalent complex; 2) nucleophilic attack operated by a tyrosine residue (Tyr723) on one DNA strand with the formation of 3′-phosphotyrosine bond; 3) strand rotation of the intact strand around the nicked strand to resolve the supercoil; 4) religation of the DNA strand; and 5) enzyme release [4]. hTop1B is the unique molecular target of a class of anticancer compounds belonging to the camptothecin family (CPTs) [5], which are able to interact with the protein–DNA covalent complex only once the cleavage has occurred, slowing down the religation step [6,7]. The parental compound, extracted from the plant *Camptotheca acuminata*, is poorly soluble and toxic for the organisms. A series of derivatives have been developed and two of them, topotecan (TPT) and irinotecan, are in clinical use for the cure of ovarian, breast, lung and colorectal cancers [7,8].

The 3D structure of the protein has been solved both in covalent and non-covalent complex with a 22 bp DNA substrate [9]. The enzyme is composed of 1) a N-terminal domain (residues 1–214) that, due to its high degree of flexibility, has never been crystallized, dispensable for the catalytic activity and deputed to the nuclear localization and interaction with other proteins; 2) a core domain (residues 215–635) further divided in subdomains I, II and III (Fig. S1A, yellow, blue and red respectively); 3) a C-terminal domain (residues 713–765) containing the catalytic residue Tyr723 (Fig. S1A, cyan) and 4) a linker domain (residues 636–712) connecting subdomain III with the C-terminal (Fig. S1A, green) [9,10]. The linker domain, formed by two long helices, protrudes out of the globular shape of the protein and it is directly involved in the relaxation mechanism since, due to its shape and its positive charge, it interacts with the DNA substrate downstream the cleavage site driving the relaxation through a "controlled rotation" mechanism [4]. The importance of the domain in modulating the activity and the reactivity to the drug has been demonstrated by its deletion that gives rise to a still active enzyme, characterized by an increased religation rate and a partial CPT resistance [11]. The linker deleted enzyme loses the motion correlation between the various protein domains, that is likely needed for the correct functioning of the enzyme, as demonstrated by MD simulations [12,13]. Biochemical and MD studies, carried out on single and double mutants, have confirmed that modulation of the linker flexibility also

Abbreviations: hTop1B, human topoisomerase 1B; CPT, camptothecin; TPT, topotecan; DMSO, dimethyl sulfoxide; EDTA, ethylenediaminetetraacetic acid; EGTA, ethylene glycol tetraacetic acid; DTT, dithiothreitol; BSA, bovine serine albumin; TBE, tris-borate-EDTA; PMSF, phenylmethanesulfonylfluoride

* Corresponding author at: Department of Biology, University of Rome Tor Vergata, Via Della Ricerca Scientifica, Rome 00133, Italy.
E-mail address: desideri@uniroma2.it (A. Desideri).

[1] These authors contributed equally to the work.

1570-9639/$ – see front matter © 2013 Elsevier B.V. All rights reserved.
http://dx.doi.org/10.1016/j.bbapap.2013.09.017

perturbs the inter-domain correlation and the reactivity of the enzyme toward anticancer drugs [14–19]. The correlation between the linker and the drug reactivity is confirmed by the fact that the linker and part of the 629–640 loop connecting the linker to subdomain III are not always observed in the X-ray structure of the protein–DNA binary complex, while are always detectable in the structures of the protein–DNA–drug ternary complexes [6,9,20,21]. In the case of the 629–640 residues, two amino acids, His632 and Arg634, form stable hydrogen bonds with DNA, as observed in the X-ray structures and in all the investigated MD simulations [6,9,15,16,18,20–23]. His632, that belongs to the catalytic pentad (Arg488, Lys532, Arg590, His632, and Tyr723), interacts with both the −1 and with the +2 bases of the scissile strand, while Arg634, that is a residue well conserved among the different organisms (Supplementary Fig. S1B), interacts with the +2 base of the scissile strand. The occurrence of such hydrogen bonds likely influences the linker flexibility and so the enzyme function and CPT reactivity. This hypothesis can be tested upon their mutation that however cannot be done on His632 that, belonging to the catalytic pentad, has a direct role on the enzyme activity.

In this work the role of Arg634 in affecting the linker mobility, via its interaction with DNA, has been investigated through an arginine to alanine mutation, analyzing the activity and drug sensitivity of the mutant using in vitro biochemical assays. A comparative molecular dynamics simulation of the wild type and mutant proteins has been carried out in order to detect the structural and dynamical effects of the mutation. The results confirm a strategic role of Arg634 in modulating the linker flexibility and the protein function and the concomitant experimental and simulative approaches provide an explanation for this behavior.

2. Materials and methods

2.1. Chemicals, yeast strains and plasmids

DMSO and CPT were purchased from Sigma-Aldrich. CPT was dissolved in 99.9% DMSO to a final concentration of 4 mg/ml (11.5 mM) and stored at −20 °C.

ANTI-FLAG M2 monoclonal affinity gel, FLAG peptide and ANTI-FLAG M2 monoclonal antibody were purchased from Sigma-Aldrich.

Saccharomyces cerevisiae top1 null strain EKY3 (ura3-52, his3Δ200, leu2Δ1, trp1Δ63, top1::TRP1, MATα) was used to express the hTop1B gene. YCpGAL1-e-hTop1B single copy plasmid was described previously [24]. Arg634Ala was generated by oligonucleotide-directed mutagenesis of the YCpGAL1-hTop1B in which the hTop1B is expressed under the galactose inducible promoter in a single-copy plasmid. The epitope-tagged construct YCpGAL1-e-hTop1B contains the N-terminal sequence FLAG: DYKDDDDY (indicated with 'e'), recognized by the M2 monoclonal antibody. The epitope-tag was subcloned into YCpGAL1-hTop1BArg634Ala to produce the YCpGAL1-e-hTop1BArg634Ala. The cloning reactions were transformed into XL10-Gold *E. coli* cells (Agilent Technologies) and positive clones were identified by sequencing the extracted plasmid DNA.

2.2. Drug sensitivity assay

Yeast EKY3 strains were transformed with YCp50, YCpGAL1-e-hTop1B and YCpGAL1-e-hTop1BArg634Ala vectors by LiOAc treatment [25] and selected on synthetic complete (SC)-uracil medium supplemented with 2% dextrose. Transformants were grown to an A595 = 0.3 and 5 μl aliquots of serial 10-fold dilutions were spotted onto SC-uracil plates plus 2% dextrose or 2% galactose, with or without the indicated concentrations of CPT.

2.3. hTop1B and hTop1BArg634Ala purification

EKY3 yeast cells, transformed with the YCpGAL1-e-hTop1B and YCpGAL1-e-hTop1BArg634Ala, were grown overnight on SC-uracil plus 2% dextrose, at an optical density of A595 = 1.0 and they were diluted 1:100 in SC-uracil plus 2% raffinose. Cells were induced with 2% galactose for 6 h at an optical density of A595 = 1.0. Cells were then centrifuged, washed with cold water and resuspended in 2 ml buffer/g cells [50 mM Tris–HCl, pH 7.4, 1 mM EDTA, 1 mM EGTA, 10% glycerol and protease inhibitors cocktail from Roche, supplemented with 0.1 mg/ml sodium bisulfate, 0.8 mg/ml sodium fluoride, 1 mM Phenylmethanesulfonylfluoride (PMSF) and 1 mM DTT]. After addition of 0.5 volumes of 425–600 μm diameter glass beads, the cells were disrupted by vortexing for 30 s alternating with 30 s on ice and then centrifuged at 15,000 *g* for 30 min. For homogenous protein preparations, the whole extracts were applied to an ANTIFLAG M2 affinity gel (Sigma-Aldrich) already equilibrated according to the manufacturer protocol. Columns were then washed with 20 volumes of TBS (50 mM Tris–HCl pH 7.4 and 150 mM KCl) supplemented with the protease inhibitors, prior to load the lysate. Elution of e-hTop1B or e-hTop1BArg634Ala, was performed by competition with five column volumes of a solution containing 1 mg of FLAG peptide (DYKDDDDK) in TBS. Fractions of 500 μl were collected and 80% glycerol was added in all preparations, which were stored at −20 °C [15]. Protein levels and integrity were assessed by immunoblot with the monoclonal anti M2 antibody (Sigma-Aldrich). The hTop1B and hTop1BArg634Ala similar concentrated fractions were also compared to the purified hTop1B with a known concentration (provided from Topogen) by immunoblot using the ab58313 Anti-hTop1B antibody (Abcam) and ab97240 goat polyclonal secondary antibody (Abcam). The relative concentrations of the two chosen fractions were estimated by a densitometry quantification using ImageJ software. The in vitro experiments have been performed using equal amount of purified hTop1B and hTop1BArg634Ala.

2.4. DNA relaxation assays

The activity of 1 μl of hTop1B (24 ng/μl) or hTop1BArg634Ala (24 ng/μl) was assayed in 30 μl of reaction volume containing 0.5 μg of negatively supercoiled pBlue-Script KSII(+) DNA, that is present in both dimeric and monomeric forms, and reaction buffer (20 mM Tris–HCl pH 7.5, 0.1 mM Na_2EDTA, 10 mM $MgCl_2$, 5 μg/ml acetylated bovine serum albumin and 150 mM KCl). The effect of CPT on enzyme activity was measured by adding DMSO or 100 μM of the drug to the reactions that were stopped with 0.5% SDS after each time-course point at 37 °C. The samples were resolved in a 1% (w/v) agarose gel in 48 mM Tris, 45.5 mM boric acid, 1 mM EDTA at 10 V/cm. The gels were stained with ethidium bromide (0.5 μg/ml), destained with water and photographed using a UV transilluminator. To quantify the disappearance of the bands due to the supercoiled DNA, the stained gels were first exposed to UV light for 30 min, to induce photo-nicking of the DNA, then restained with ethidium bromide (0.5 μg/ml) for 20 min [17]. Bands corresponding to supercoiled DNA were quantified using the ImageJ software (http://rsbweb.nih.gov/ij/), normalized to the total amount of DNA present in each lane and plotted as function of time.

2.5. Cleavage kinetics

Oligonucleotide CL14-U (5′-GAAAAAAGACTUAG-3′) containing an hTop1B high affinity cleavage site, was 5′ end labeled with [γ 32P] ATP. The CP25 complementary strand (5′-TAAAAATTTTTCTAAGTC TTTTTTC-3′) was 5′-end phosphorylated with unlabeled ATP. The two strands were annealed with a 2-fold molar excess of CP25 over CL14U. 20 nM substrate has been incubated with an excess of hTop1B or hTop1BArg634Ala enzymes in 20 mM Tris–HCl pH 7.5, 0.1 mM Na_2EDTA, 10 mM $MgCl_2$, 5 μg/ml acetylated BSA, 150 mM KCl, at 25 °C in a final volume of 50 μl. At various time points 5 μl aliquots were removed and the reaction stopped with 0.5% (w/v) SDS and directly loaded without ethanol precipitation and trypsin digestion. Samples have been analyzed by denaturing 7 M urea/20% polyacrylamide gel electrophoresis in TBE

(48 mM Tris, 45.5 mM Boric Acid, 1 mM EDTA). The percentage of cleaved substrate (Cl1) was determined by PhosphorImager and ImageQuant software and normalized on the total amount of radioactivity in each lane.

2.6. Religation kinetics

Oligonucleotide CL14 (5′-GAAAAAAGACTTAG-3′) containing a hTop1B high affinity cleavage site was 5′-end labeled with [γ 32P] ATP. The CP25 complementary strand (5′-TAAAAATTTTTCTAAGTCTTTTTTC-3′) was 5′-end phosphorylated with unlabeled ATP. The two strands were annealed with a 2-fold molar excess of CP25 over CL14 [26].

20 nM of CL14/CP25 (suicide substrate) was incubated with an excess of hTop1B or hTop1BArg634Ala for 60 min at 25 °C followed by 30 min at 37 °C in 20 mM Tris–HCl pH 7.5, 0.1 mM Na_2EDTA, 10 mM $MgCl_2$, 50 μg/ml acetylated BSA, and 150 mM KCl [11]. After the formation of the cleavage complex (Cl1p) a 5 μl aliquot was removed and used as time 0 point, then DMSO or 100 μM CPT were added and religation reaction was started by adding a 200-fold molar excess of R11 oligonucleotide (5′-AGAAAAATTTT-3′) over the CL14/CP25 [11]. 5 μl aliquots were removed at various time points, and the reaction stopped with 0.5% SDS. After ethanol precipitation, samples were resuspended in 5 μl of 1 mg/ml trypsin and incubated at 37 °C for 60 min. Trypsin doesn't digest hTop1B completely so a trypsin resistant peptide remains attached to the substrate causing the 12 nt (Cl1p) oligo to run slower than the uncleaved in the gel. Samples were analyzed by denaturing 7 M urea/20% polyacrylamide gel electrophoresis in 48 mM Tris, 45.5 mM Boric Acid, 1 mM EDTA. The percentage of remaining cleavage complex was quantified by ImageQuant software, normalized to the total radioactivity for each lane and to the value at $t = 0$ and finally plotted as a function of time.

2.7. Molecular dynamics

Molecular dynamics simulation of the hTop1B-DNA covalent complex has been carried out. The starting coordinates of the protein residues 201–765 and of the 22 bp DNA molecules have been obtained as described in Mancini et al. 2012 [22]. The mutation of residue Arg634 to alanine has been directly introduced with the tleap module of Amber 12 [27] during the building of the topology. The wild type and mutant complexes have been immersed in a triclinic box filled with TIP3P water molecules [28] and rendered neutral by the addiction of 22 and 21 Na^+ counterions. The topologies have been created using tleap with the ff99bsc0 Amber force field [29]. The Amber topologies have been then converted in the Gromacs v. 4.5 format using Acpype [30,31]. The simulations have been then carried out using Gromacs. Electrostatic interactions have been taken into account by means of the Particle Mesh Ewald method [32] and the SHAKE algorithm [33] has been used to apply a constraint on all hydrogen bond length. Optimization and relaxation of solvent and ions were initially performed keeping the protein–DNA atoms constrained to their initial position with decreasing force constants of 1000 and 500 kJ/(mol·nm), for 500 ps. The system has then been simulated for 75 ns at a constant temperature of 300 K using the Berendsen's method [34] and at a constant pressure of 1 bar; the pressure was kept constant (1 bar) using the Rahman–Parrinello barostat [35] with a 2.0 fs time step. All the analyses have been performed with the GROMACS MD package v. 4.5 [30], images were obtained with the VMD program [36] and graphs with the Grace program.

The analyses have been performed considering the last 72 ns of simulation, once eliminated the equilibration time, and have been compared to a previously performed simulation of the human wild type enzyme [22].

3. Results

3.1. The Arg634Ala mutant is active and resistant to CPT when expressed in yeast cells

In *Saccharomyces cerevisiae*, where the Top1 gene isn't essential, camptothecin sensitivity of ΔTop1 yeast cells can be introduced expressing human Top1 gene [37]. The effect of the Arg634Ala mutation has been tested in a viability assay on a Top1Δ yeast strain (EKY3), transformed with GAL1-e-hTop1B constructs (Fig. 1). At least five independent clones were selected from each transformation. Serial dilutions of yeast cells, transformed with the indicated plasmids, have been spotted on plates containing dextrose, to assess the general growth, or galactose, to monitor the effect of the inducible expression of the enzymes. Yeast cells are fully viable in dextrose while galactose slightly affects the viability (top of Fig. 1).

The same yeast cells have been spotted on galactose plates supplemented with CPT concentration from 5 to 500 ng/mL (bottom of Fig. 1), to test the CPT sensitivity when the expression of hTop1B is induced. Yeast cells, expressing wild type hTop1B, show growth deficiency in the presence of 10 ng/mL of CPT, while yeasts containing the Arg634Ala mutant produce viable colonies up to a concentration of 100 ng/mL, indicating that the mutation confers resistance to the drug. Yeasts transformed with the "empty" vector, used as control, show no response to CPT as expected.

3.2. The mutant Arg634Ala is resistant to CPT in vitro

The ability of wild type and Arg634Ala enzymes to relax a supercoiled plasmid has been investigated in the absence and presence of 100 μM CPT at physiological condition of 150 mM KCl. Equal amounts of purified proteins have been incubated with 0.5 μg of a negative supercoiled plasmid in a time course experiment from 0.16 to 30 min (Fig. 2A). The assay in the absence of CPT has been carried out in the presence of DMSO to control that the CPT solvent doesn't affect the relaxation activity of the two enzymes. The products have been resolved by agarose gel electrophoresis (Fig. 2A). The amount of supercoiled DNA has been quantified, normalized to the total amount of DNA for each lane and plotted as a function of time (Fig. 2B).

The supercoiled DNA is completely relaxed by the wild type after 4 min (Fig. 2A lane 7) while the mutant is slightly faster, completely relaxing the supercoiled DNA after 2 min (Fig. 2A lane 6). In the presence of CPT the relaxation rate decreases. In detail, CPT inhibits the relaxation rate of wild type up to 30 min (Fig. 2A lane 19), while in the case of the Arg634Ala mutant the inhibition is present only up to 8 min (Fig. 2A lane 17). Quantification of the disappearance of the bands, corresponding to supercoiled DNA, evidences that the two proteins have almost the same relaxation rate in the absence of the drug (Fig. 2B, compare black and gray full lines in the graph) while the mutant displays a faster relaxation rate in the presence of CPT (Fig. 2B, compare black and gray dashed lines in the graph). This result indicates that the mutant is also resistant to CPT when it is purified.

3.3. Kinetics of cleavage of the wild type and Arg634Ala mutant

The time course of the cleavage of the wild type and Arg634Ala mutant has been followed using a suicide cleavage substrate made by a 5′-end radiolabeled oligonucleotide CL14-U (5′-GAAAAAAGACTUAG-3′) having a ribo-Uracil (rU) in position 12 (top of Fig. 3A), annealed to a CP25 (5′-TAAAAATTTTTCTAAGTCTTTTTTC-3′) complementary strand, to produce a duplex with an 11-base 5′-single-strand extension. The enzyme cuts the substrate at the preferred site close to the uracil, indicated by an arrow in Fig. 3A. After the cutting, the 2′-OH of the ribose can attack the 3′-phosphotyrosyl linkage between the enzyme and ribonucleotide, permitting the release of hTop1B leaving a 2′,3′-cyclic phosphate end [38].

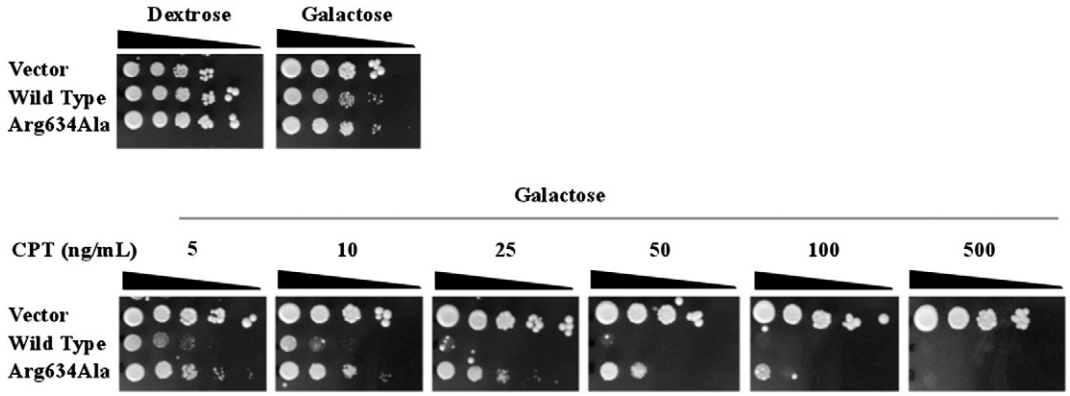

Fig. 1. Yeast cell viability assay. Exponentially growing yeast cells transformed with a single copy plasmid expressing vector, wild type and Arg634Ala have been serially 10-fold diluted and spotted onto selective media in the presence of dextrose, galactose, or galactose plus the indicated CPT concentrations.

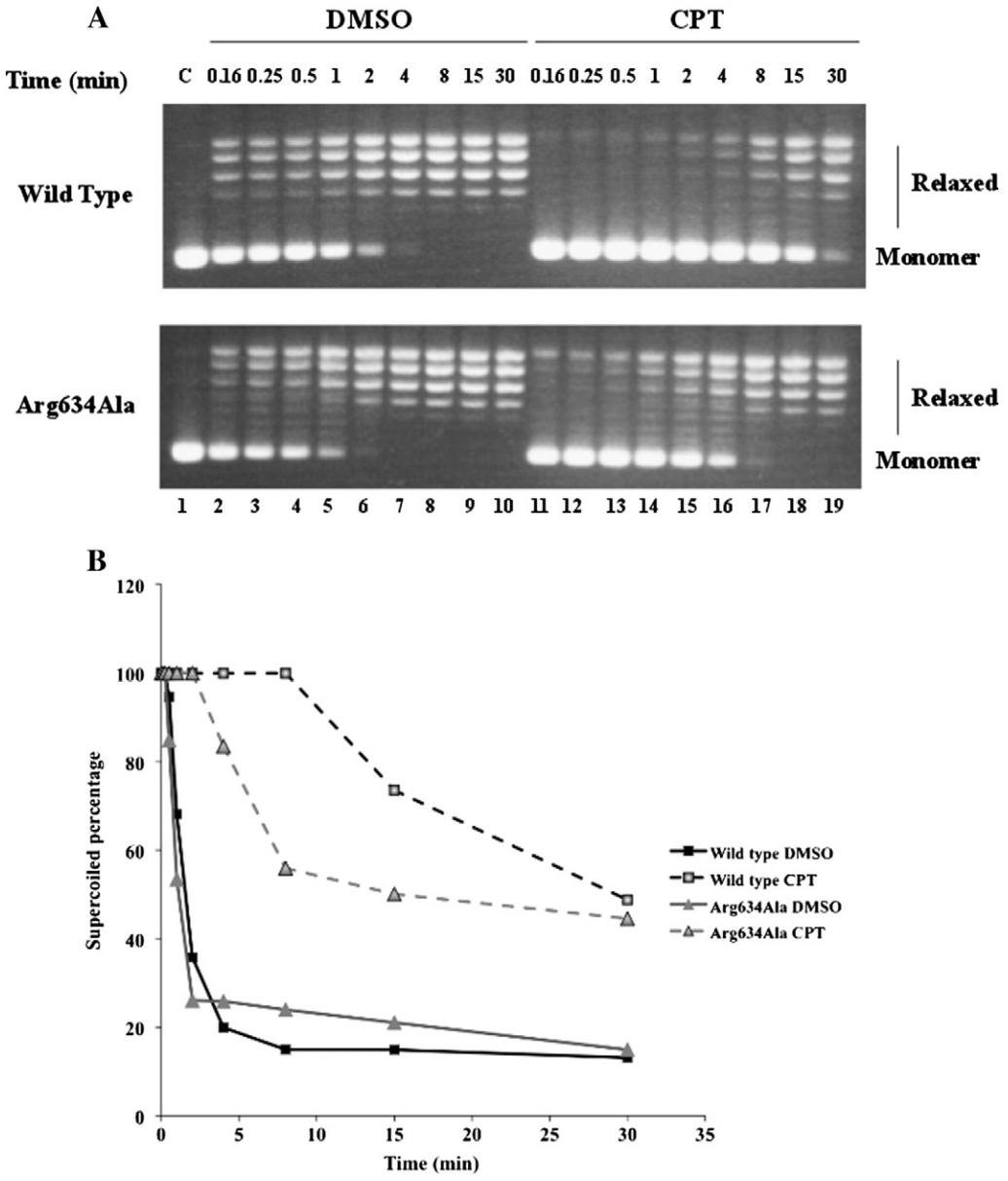

Fig. 2. Relaxation of supercoiled DNA. (A) Relaxation of negative supercoiled plasmid in a time course experiment for the wild type and the Arg634Ala mutant in presence of DMSO (lanes 2–9) and 100 μM CPT (lanes 10–19); lane 1 represents the control (C) where no protein is added. The reaction products are resolved in agarose gel and visualized with ethidium bromide. The two forms of the plasmid DNA are indicated as "monomer" and "relaxed". (B) Percentage of supercoiled DNA, relative to the total amount of DNA for each lane, plotted against time in absence or in presence of CPT for the wild type (squares, full and dashed black lines, respectively) and the Arg634Ala mutant (diamonds, full and dashed gray lines, respectively).

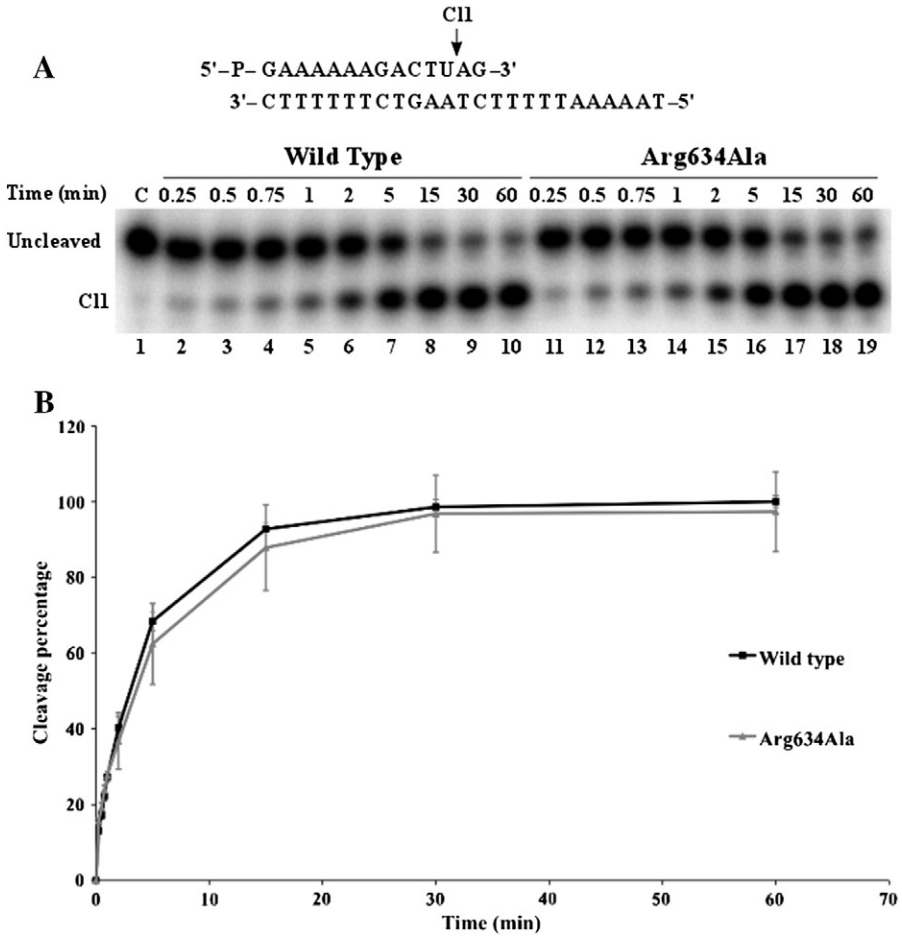

Fig. 3. Cleavage kinetics using ribo-modified substrate. (A) Time course (0.25–60 min) of the cleavage reaction of purified wild type (lanes 2–9), and Arg634Ala mutant (lanes 10–19) with the CL14-U/CP25 substrate (shown at the top of the figure). In lane 1 the protein has not been added. CL1 represents the DNA strand cleaved by the enzymes at the preferred cleavage site, indicated by an arrow at the top of the figure. (B) Percentage of cleaved substrate, normalized to the maximum value of the wild type, plotted against time for the reaction with wild type (black squares) and with Arg634Ala mutant (gray diamonds). Data shown are means ± SD from at least 3 independent experiments.

An excess of wild type and mutant enzymes have been incubated with the substrate to obtain the cleaved DNA fragments that have been resolved in a denaturing polyacrylamide gel, shown in Fig. 3A. The amount of cleaved fragment, normalized to the plateau value of the wild type protein and plotted as a function of time, shows that the wild type protein and the Arg634Ala mutant have the same rate of cleavage and reach the same plateau value (Fig. 3B).

3.4. Kinetics of religation of the wild type and Arg634Ala mutant

A direct measure of the religation rate has been carried out using the oligonucleotide substrate CL14 (5′-GAAAAAAGACTTAG-3′), containing a preferred cleavage site for hTop1B, radiolabeled at its 5′ end and annealed to the CP25 complementary strand (5′-TAAAAATTTTTCTAA GTCTTTTTTC-3′) to generate a suicide cleavage substrate [11]. HTop1B cut this substrate at the preferred site, indicate by an arrow in Fig. 4A, but the religation step is excluded because the generated AG-3′ dinucleotide is too short to be religated and the enzyme remains covalently attached to the 12 oligonucleotide 3′ end.

The suicide cleavage substrate has been incubated with an excess of wild type and mutant enzymes to allow the cleavage to proceed to completion. A 200-fold molar excess of complementary R11 oligonucleotide (5′-AGAAAAATTTT-3′) has been then added in absence and presence of CPT and aliquots have been removed and analyzed at different times on urea-polyacrylamide gel, as described in materials and methods. The percentage of the remaining covalent complex (Cl1p) has been determined, normalized to the time 0 and plotted in Fig. 4B, as routinely quantified in religation experiments [39]. The data show that the Arg634Ala mutant has a religation rate higher than the wild type enzyme (Fig. 4A, compare lanes 2–6 with lanes 11–15; Fig. 4B compare full black with full gray line). The presence of CPT strongly decreases the religation rate of the wild type protein (Fig. 4A lanes 7–10; Fig. 4B dashed black line). A decrease is also observed for the Arg634Ala mutant (Fig. 4A lanes 16–19; Fig. 4B dashed gray line), but in this case the presence of CPT brings the religation rate of the mutant to a value comparable to the one observed in the wild type in the absence of the drug, indicating that the mutant undergoes an efficient religation also in the presence of the drug.

3.5. Local effect of the Arg634Ala mutation and influence on protein flexibility

The structural and dynamical effect of the mutation, leading to an increase in the religation rate, have been investigated by molecular dynamics simulation of the wild type and mutant enzymes in covalent complex with a 22 bp DNA substrate.

Analysis of the trajectories indicates that the local effect of the mutation is detectable at the level of the hydrogen bonds network between residues 632–712 and the DNA bases as shown in Table 1, where the H-bonds present for at least 50% of total length in one of the two

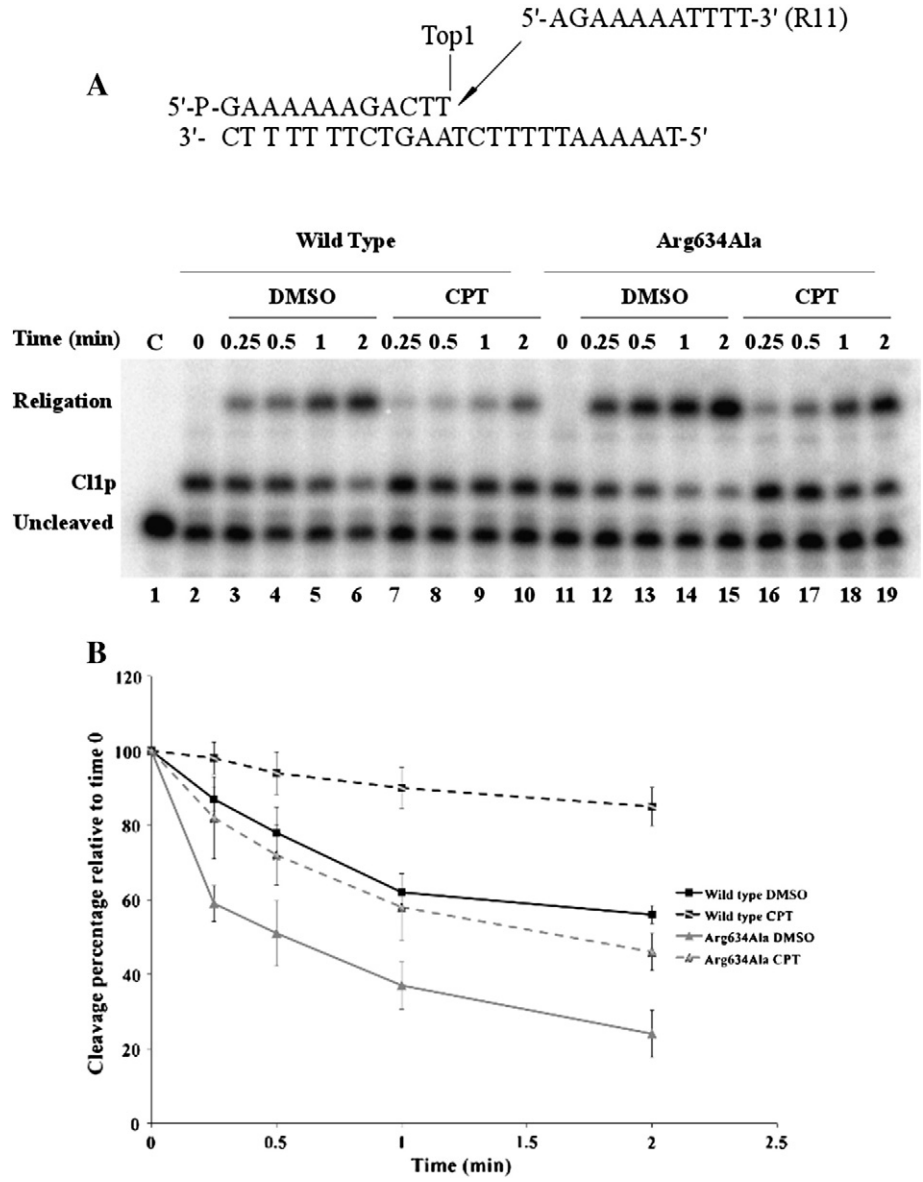

Fig. 4. Religation kinetics. (A) Gel analysis of the religation kinetics observed when incubating the wild type or the Arg634Ala mutant-suicide cleavage complex with the R11 complementary ligator oligonucleotide (shown at the top of the figure) in absence (lanes 3–6 and lanes 12–15 for wild type and Arg634Ala mutant respectively) or in presence of 100 μM CPT (lanes 7–10 for the wild type and lanes 16–19 for the Arg634Ala mutant). In lane 1 no protein was added. The lanes 2 and 11 represent the time 0 for the wild type and the Arg634Ala mutant reactions, before the addition of the complementary R11 strand. "Cl1p" represents the protein–DNA complex formed at the preferred enzyme site; "religation" is the restored fully duplex oligonucleotide representing the final product of the religation reaction. (B) Plot of the percentage of disappearance of the cleavage complex relative to time 0, in absence or in presence of CPT for the wild type (squares, full and dashed black lines, respectively) and the Arg634Ala mutant (diamonds, full and dashed gray lines, respectively). Data shown are means ± SD from 3 independent experiments.

simulations are reported. The lack of the Arg634-Gua +2 interaction in the mutant causes a rearrangement of the surrounding residues, so that the interaction of His632 with the +2 base is also lost, while new interactions between Gln633 and Ala635 with the +2 and +3 bases appear (Table 1). An additional hydrogen bond between the linker and the DNA involving the Asn646 and Gln704 residues and the +7 thymine of the intact strand also appears (Table 1).

Table 1
Percentage of occurrence of protein–DNA hydrogen bonds involving residues close to the mutation site.

	Wild type	R634A
His632-Gua +2(s)	75%	–
Gln633-Gua +2(s)	–	93%
Arg634-Gua +2(s)	81%	–
Ala635-Ade +3(s)	–	92%
Asn646-Ade +8(i)	47%	61%
Gln704-Thy +7(i)	10%	71%
Arg708-Thy +7(i)	57%	54%

Hydrogen bonds between the DNA and residues 629–712 found for at least 50% of total simulation time in one of the two trajectories are reported. s = scissile, i = intact.

The mutation has also an effect on the whole protein flexibility. Overall, the two proteins show a similar profile of fluctuation, as evidenced by the plot of the per-residue Root Mean Square Fluctuation (RMSF) reported in Fig. 5, although the linker domain, the C-terminal domain and the final portion of subdomain III display a lower flexibility degree in the mutant (Fig. 5). The decreased mobility of the C-terminal domain is coupled to an increased fluctuation of the 718–723 residues, containing the catalytic Tyr723 and Asn722, involved in the stabilization of the drug through a water mediated hydrogen bond, as evidenced by the X-ray diffraction and MD simulation of the protein–DNA–drug ternary complex [6,21–23].

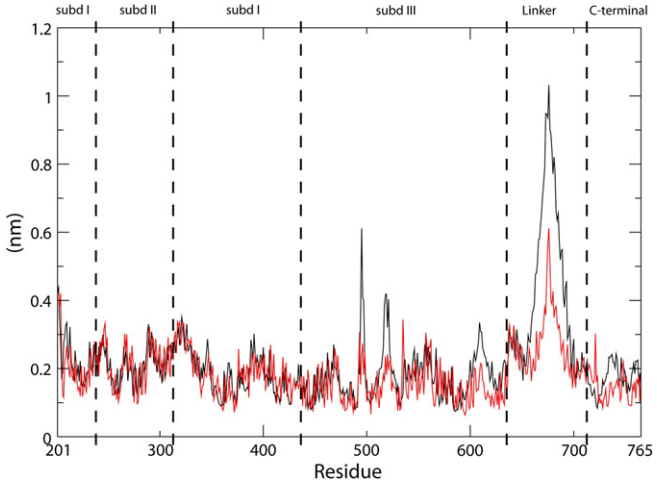

Fig. 5. Protein mobility. Per-residue Root Mean Square Fluctuation (RMSF) of the wild type (black line) and Arg634Ala mutant (red line). The domain subdivision is reported.

3.6. The mutation destabilizes the CPT binding site

The three-dimensional structure of the hTop1B–DNA–CPT ternary complex has shown that the drug, besides being stacked with the −1/+1 nucleotides, is maintained in its position by direct or water mediated hydrogen bonds established with residues Arg364, Asp533 and Asn722 [6] (Fig. 6A). The importance of these interactions is confirmed by the fact that point mutation of these residues is associated to drug resistance [40–42]. These residues are also involved in the stabilization of other drugs such as topotecan, indenoisoquinolines and indolocarbazoles, and the importance of their interaction with the drug has also been highlighted by MD simulation [22,23]. The three-dimensional arrangement of these three residues is identical both in the hTop1B–DNA binary and the hTop1B–DNA–drug ternary complexes, as evidenced by X-ray diffraction (Fig. 6A and B) [6,9,20,21], suggesting that the drug binding site is pre-formed and ready to accommodate it. In line, the orientation of the three residues is maintained along the entire trajectory in the simulation of the wild type enzyme (Fig. 6C). On the other hand, in the simulation of the Arg634Ala mutant the orientation of the lateral chains of the CPT binding residues is different (Fig. 6D), due to a rearrangement in the hydrogen bonds, reported in Table. 2, established by Arg364, Asp533 and Asn722 with the surrounding residues and with the DNA bases, that have been shown to play an important role in stabilizing the drug [43]. In detail, the hydrogen bond network detected in the wild type is disrupted in the mutant, indicating that the mutation of Arg634 has an effect on the protein–DNA interaction not only in proximity of the mutation, but also on the orientation of the lateral chains of Arg364, Asp533 and Asn722, bringing to the disruption of the pre-formed drug binding site observed in the wild type, so in part explaining the partial CPT resistance observed in the mutant.

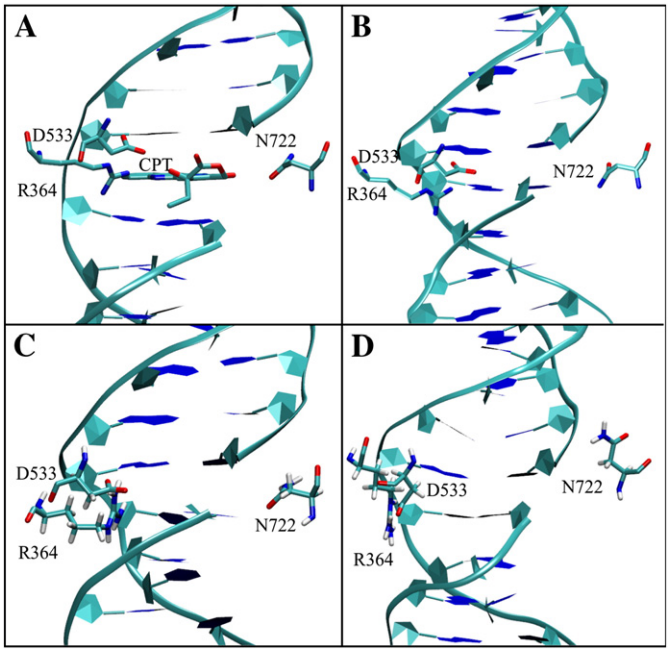

Fig. 6. CPT binding site analysis. (A) hTop1B–DNA–CPT X-ray structure (PDB ID 1T8I), (B) hTop1B–DNA X-ray structure (PDB ID 1A31) and representative snapshot for (C) the wild type and (D) the Arg634Ala mutant simulation, of the CPT binding site residues and of the DNA substrate. In (A) the CPT is also present.

3.7. Residue correlation map

The effect of the mutation on the protein domains motion has been analyzed calculating the Dynamic Cross Correlation (DCC) map of the Cα atoms of the whole protein (Fig. 7). For each couple of residues, the map defines whether their motion is positively correlated (same direction and orientation), negatively correlated (same direction and opposite orientation) or completely uncorrelated. In the map reported in Fig. 7 the cyan to magenta points indicate the occurrence of an increasing negative correlation, the green to red points an increasing positive correlation and the gray and white points small or absent correlation. The mutant enzyme (bottom right area of Fig. 7) is characterized by a degree of correlation much lower than the wild type (top left area of Fig. 7). In detail, in the wild type a strong correlated motion between subdomain I and subdomains II and III is observed (Fig. 7, top left, A and B rectangles). In the mutant the correlation between subdomains I and II is partially maintained (Fig. 7, bottom right, C rectangle), while the one with subdomain III is completely lost. More importantly, in the wild type the linker domain is strongly correlated with the terminal region of subdomain III and with the C-terminal domain (Fig. 7, top left, D and E rectangles). In the mutant enzyme there is a complete lack of correlation between these regions (Fig. 7, bottom right). It is interesting that a similar loss of the correlation has been also observed in the Thr729Lys and Glu710Gly CPT resistant mutant [16,44].

The confinement of the motion of the linker, and of the whole mutated protein, in a reduced space is also evidenced by the analysis of the principal components of the motion (PCA). In the wild type enzyme 60% of total motion is represented by the first 6 eigenvectors while in the mutant the same percentage is already covered by the first 3 eigenvectors. Projection of the motion along the plane formed

Table 2
Percentage of occurrence of the hydrogen bonds involving residues composing the CPT binding site in the wild type.

	Wild type	R634A
Arg364-Asp533	98%	57%
Arg364-Cyt +1(i)	35%	68%
Arg364-Ade −1(i)	92%	53%
Arg364-Ade −2(i)	100%	83%
Arg364-Gua +1(s)	70%	–
Arg364-Gua +2(s)	80%	–
Lys532-**Asp533**	86%	–
Asp533-Gua −3(i)	82%	–
Thr591-**Asn722**	–	60%
Tyr723-**Asn722**	–	65%
Asn722-Thy −1(s)	96%	–

The interactions found for at least 50% of total simulation time in one of the two trajectories are reported. s = scissile, i = intact. Residues forming the CPT binding site in the wild type are evidenced in bold.

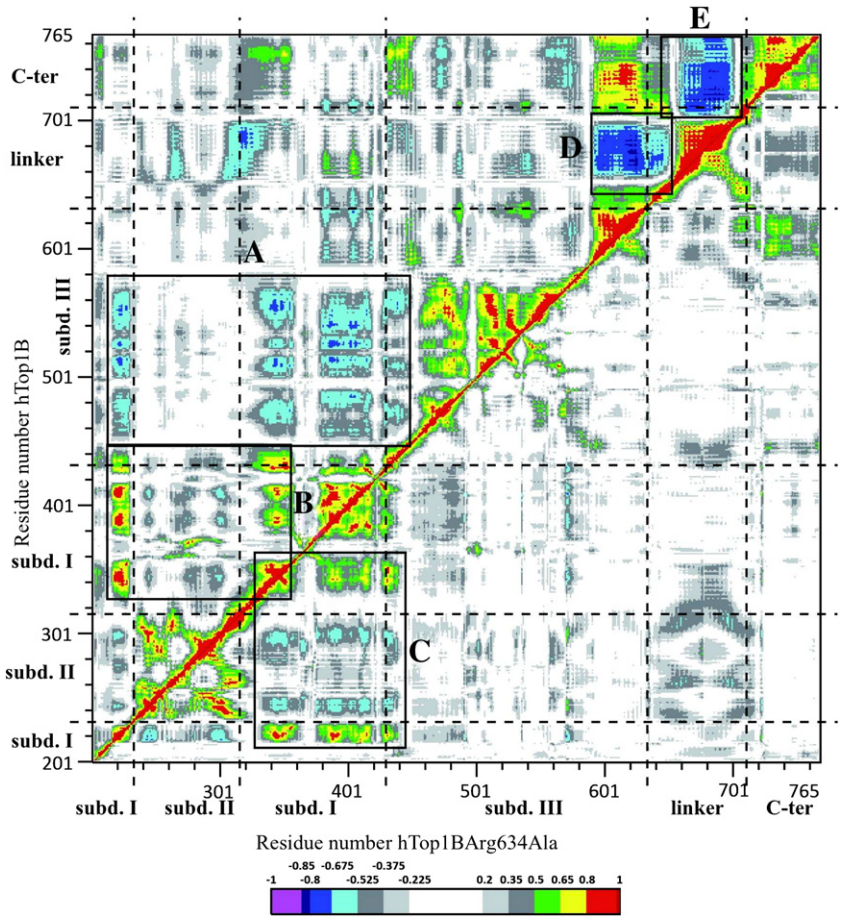

Fig. 7. Correlated motions. Dynamic Cross Correlation (DCC) map of the wild type (top left area) and of the Arg634Ala mutant (bottom right area). The color scale is also reported. The rectangles highlight the regions with the highest degree of correlation in each simulation.

by the first 2 eigenvectors highlights the different protein mobility. The amplitude of the motion along the first and the second eigenvectors for the wild type is 170 and 116 Å, respectively, while in the mutant the amplitude along the same eigenvectors is 109 and 93 Å, respectively (Fig. S2, black vs red points).

4. Discussion

The viability assay carried out on yeast cells lacking the endogenous Top1B and transformed with the hTop1B indicates that the cells expressing the Arg634Ala mutant display CPT resistance, being able to grow also in presence of 100 ng/ml of CPT (Fig. 1). Characterization of the different steps of the catalytic cycle of the Arg634Ala mutant permits to understand the basis for its resistance. The mutant has a relaxation rate comparable to the wild type in the absence of the drug (Fig. 2B, full gray and black lines, respectively) but addition of CPT only partially affects its relaxation (Fig. 2B, dashed gray and black lines, respectively). The mutant and the wild type also have an identical cleavage rate, as shown by the experiments reported in Fig. 3, but the mutation has a direct effect on the religation rate that it is at least two times faster in the mutant than in the wild type (Fig. 4). Addition of CPT strongly reduces the native enzyme religation rate giving rise to the already reported poisoning effect. CPT also reduces the mutant religation rate but in this case the observed rate is almost identical to the one observed in the native enzyme in the absence of the drug, thus explaining the drug resistance displayed by the mutant (Fig. 4).

In order to understand at atomic level which are the structural–dynamical effects of the mutation leading to drug resistance a comparative molecular dynamics simulation of the wild type and Arg634Ala mutant in covalent complex with a 22 bp DNA substrate have been carried out. The analysis shows local effects of the mutation detectable at the level of the hydrogen bonds established by the loop containing the 634 residue (residues 629–640), that connects subdomain III with the linker domain, and by the linker with DNA (Table 1). This rearrangement is correlated to a different protein flexibility, the mutant in fact shows a lower degree of flexibility at the level of the linker, C-terminal domain and of the terminal region of subdomain III (Fig. 5) with a consequent loss of motion correlation between the different protein domains when compared to the wild type (Fig. 7). In detail, the linker domain loses the correlated motion with subdomain III and with the C-terminal domain when compared to the wild type (Fig. 7, compare top left with bottom right areas), likely impairing the correct motion of the protein domains during the controlled rotation and further religation reaction (Fig. 4).

The loss of correlated motions may explain the increased relaxation/religation rate of the mutant either in absence or in presence of camptothecin (Figs. 2 and 4), confirming the crucial role of the linker in controlling the rotation/religation process [4]. The importance of this domain has been stated by several works carried out on a linker-deleted enzyme or on protein carrying point mutations at the level of the domain [11,13–15,18,19]. In a pioneering work Champoux and colleagues have demonstrated that a linker-deleted protein displays an increased religation rate and partial CPT resistance [11]. A correlation between large linker conformational variability, increased religation rate and CPT insensitivity has been reported for the single Ala653Pro mutation and more recently for a chimeric enzyme where the human linker has been substituted with plasmodial one [14,45]. CPT resistance has been also reported for the Thr729Lys mutant, characterized by

comparable linker flexibility with the wild type, but where the linker domain loses motion correlation with the other protein domains and in particular with the C-terminal domain containing the catalytic Tyr723 residue [16,17]. In the here studied Arg634Ala mutant the substitution brings to a reduction of the linker flexibility and to a complete loss of motion correlation between the linker and the C-terminal domain (Figs. 5 and 7) and from the functional point of view to an increased relaxation and religation rate and to CPT resistance. This study then confirms that perturbation of the linker has a direct effect on the catalytic function and on the drug reactivity and we propose that the occurrence of the motion correlation of the linker domain with the C-terminal domain is a necessary requisite to have the "controlled rotation" and a CPT sensitive enzyme. The increased religation rate of the mutant (Fig. 4) coupled to an identical cleavage rate (Fig. 3) explains the in vivo CPT resistance since the number of hTop1–DNA cleavage complexes is lower in the yeast hosting the mutated than the wild type enzyme.

Finally, the presence of an alanine in position 634 also affects the three-dimensional orientation of the Arg364, Asp533 and Asn722 residues forming the CPT binding site in the wild type protein (Fig. 6). The different orientation of the lateral chains of these three residues can be considered as an additional cause for a lowered stabilization of the CPT between the −1 and +1 bases, leading to partial resistance.

5. Conclusions

In conclusion, using a combined experimental and computational approach we have shown that mutation of arginine 634 to alanine of hTop1B impairs the flexibility of the linker domain, affecting the motion correlation between the linker and the other protein domains present in the wild type enzyme. The loss of interdomain communications is correlated to a faster religation rate and to partial drug resistance.

The combined biochemical and simulative approaches permits to demonstrate that mutation far from the active site affects the function of the protein and its reactivity to the drug and disrupts protein domain motion correlation, highlighting the importance of concerted domains motion for the correct function of the enzyme.

Supplementary data to this article can be found online at http://dx.doi.org/10.1016/j.bbapap.2013.09.017.

Acknowledgements

This work was supported by Associazione Italiana Ricerca Cancro (AIRC) with the project N. 10121. The authors thank Fabio Retico for the help in obtaining the simulation of the mutant. Calculations facilities to run the simulations where made available by Cineca Consortium through the Iscra C project with code IscraC_Stra-Top.

References

[1] J.J. Champoux, DNA topoisomerase I-mediated nicking of circular duplex DNA, Methods Mol. Biol. 95 (2001) 81–87.
[2] J.C. Wang, Cellular roles of DNA topoisomerases: a molecular perspective, Nat. Rev. Mol. Cell. Biol. 3 (2002) 430–440.
[3] K.D. Corbett, J.M. Berger, Structure, molecular mechanisms, and evolutionary relationships in DNA topoisomerases, Annu. Rev. Biophys. Biomol. Struct. 33 (2004) 95–118.
[4] L. Stewart, M.R. Redinbo, X. Qiu, W.G. Hol, J.J. Champoux, A model for the mechanism of human topoisomerase I, Science 279 (1998) 1534–1541.
[5] S. Castelli, A. Coletta, I. D'Annessa, P. Fiorani, C. Tesauro, A. Desideri, Interaction between natural compounds and human topoisomerase I, Biol. Chem. 393 (2012) 1327–1340.
[6] B.L. Staker, M.D. Feese, M. Cushman, Y. Pommier, D. Zembower, L. Stewart, A.B. Burgin, Structures of three classes of anticancer agents bound to the human topoisomerase I–DNA covalent complex, J. Med. Chem. 48 (2005) 2336–2345.
[7] Y. Pommier, Topoisomerase I inhibitors: camptothecins and beyond, Nat. Rev. Cancer 6 (2006) 789–802.
[8] Y. Pommier, DNA topoisomerase I inhibitors: chemistry, biology, and interfacial inhibition, Chem. Rev. 109 (2009) 2894–2902.
[9] M.R. Redinbo, L. Stewart, P. Kuhn, J.J. Champoux, W.G. Hol, Crystal structures of human topoisomerase I in covalent and noncovalent complexes with DNA, Science 279 (1998) 1504–1513.
[10] L. Stewart, G.C. Ireton, L.H. Parker, K.R. Madden, J.J. Champoux, Biochemical and biophysical analyses of recombinant forms of human topoisomerase I, J. Biol. Chem. 271 (1996) 7593–7601.
[11] L. Stewart, G.C. Ireton, J.J. Champoux, A functional linker in human topoisomerase I is required for maximum sensitivity to camptothecin in a DNA relaxation assay, J. Biol. Chem. 274 (1999) 32950–32960.
[12] G. Chillemi, P. Fiorani, P. Benedetti, A. Desideri, Protein concerted motions in the DNA–human topoisomerase I complex, Nucleic Acids Res. 31 (2003) 1525–1535.
[13] G. Chillemi, M. Redinbo, A. Bruselles, A. Desideri, Role of the linker domain and the 203–214 N-terminal residues in the human topoisomerase I DNA complex dynamics, Biophys. J. 87 (2004) 4087–4097.
[14] P. Fiorani, A. Bruselles, M. Falconi, G. Chillemi, A. Desideri, P. Benedetti, Single mutation in the linker domain confers protein flexibility and camptothecin resistance to human topoisomerase I, J. Biol. Chem. 278 (2003) 43268–43275.
[15] P. Fiorani, C. Tesauro, G. Mancini, G. Chillemi, I. D'Annessa, G. Graziani, L. Tentori, A. Muzi, A. Desideri, Evidence of the crucial role of the linker domain on the catalytic activity of human topoisomerase I by experimental and simulative characterization of the Lys681Ala mutant, Nucleic Acids Res. 37 (2009) 6849–6858.
[16] G. Chillemi, I. D'Annessa, P. Fiorani, C. Losasso, P. Benedetti, A. Desideri, Thr729 in human topoisomerase I modulates anti-cancer drug resistance by altering protein domain communications as suggested by molecular dynamics simulations, Nucleic Acids Res. 36 (2008) 5645–5651.
[17] C. Losasso, E. Cretaio, P. Fiorani, I. D'Annessa, G. Chillemi, P. Benedetti, A single mutation in the 729 residue modulates human DNA topoisomerase IB DNA binding and drug resistance, Nucleic Acids Res. 36 (2008) 5635–5644.
[18] I. D'Annessa, C. Tesauro, P. Fiorani, G. Chillemi, S. Castelli, O. Vassallo, G. Capranico, A. Desideri, Role of flexibility in protein–DNA–drug recognition: the case of Asp677Gly-Val703Ile topoisomerase mutant hypersensitive to camptothecin, J. Amino Acids 2012 (2012) 206083.
[19] C. Gongora, N. Vezzio-Vie, S. Tuduri, V. Denis, A. Causse, C. Auzanneau, G. Collod-Beroud, A. Coquelle, P. Pasero, P. Pourquier, P. Martineau, M. Del Rio, New topoisomerase I mutations are associated with resistance to camptothecin, Mol. Cancer 10 (2011) 64.
[20] M.R. Redinbo, L. Stewart, J.J. Champoux, W.G. Hol, Structural flexibility in human topoisomerase I revealed in multiple non-isomorphous crystal structures, J. Mol. Biol. 292 (1999) 685–696.
[21] B.L. Staker, K. Hjerrild, M.D. Feese, C.A. Behnke, A.B. Burgin Jr., L. Stewart, The mechanism of topoisomerase I poisoning by a camptothecin analog, Proc. Natl. Acad. Sci. U. S. A. 99 (2002) 15387–15392.
[22] G. Mancini, I. D'Annessa, A. Coletta, G. Chillemi, Y. Pommier, M. Cushman, A. Desideri, Binding of an indenoisoquinoline to the topoisomerase–DNA complex induces reduction of linker mobility and strengthening of protein–DNA interaction, PLoS One (2013)(in press).
[23] G. Mancini, I. D'Annessa, A. Coletta, N. Sanna, G. Chillemi, A. Desideri, Structural and dynamical effects induced by the anticancer drug topotecan on the human topoisomerase I–DNA complex, PLoS One 5 (2010) e10934.
[24] M.A. Bjornsti, P. Benedetti, G.A. Viglianti, J.C. Wang, Expression of human DNA topoisomerase I in yeast cells lacking yeast DNA topoisomerase I: restoration of sensitivity of the cells to the antitumor drug camptothecin, Cancer Res. 49 (1989) 6318–6323.
[25] C. Kaiser, S. Michaelis, A. Mitchell, Lithium Acetate Yeast Transformation, Cold Spring Harbor Laboratory Press, New York, 1994. 133–134.
[26] A.H. Andersen, E. Gocke, B.J. Bonven, O.F. Nielsen, O. Westergaard, Topoisomerase I has a strong binding preference for a conserved hexadecameric sequence in the promoter region of the rRNA gene from *Tetrahymena pyriformis*, Nucleic Acids Res. 13 (1985) 1543–1557.
[27] D.A. Case, T.E. Cheatham 3rd, T. Darden, H. Gohlke, R. Luo, K.M. Merz Jr., A. Onufriev, C. Simmerling, B. Wang, R.J. Woods, The Amber biomolecular simulation programs, J. Comput. Chem. 26 (2005) 1668–1688.
[28] W.L. Jorgensen, J. Chandrasekhar, J.D. Madura, R.W. Impery, M.L. Klein, Comparison of simple potential functions for simulating liquid water, J. Chem. Phys. 79 (1983) 926–935.
[29] Y. Duan, C. Wu, S. Chowdhury, M.C. Lee, G. Xiong, W. Zhang, R. Yang, P. Cieplak, R. Luo, T. Lee, J. Caldwell, J. Wang, P. Kollman, A point-charge force field for molecular mechanics simulations of proteins based on condensed-phase quantum mechanical calculations, J. Comput. Chem. 24 (2003) 1999–2012.
[30] B. Hess, C. Kutzner, van der Spoel D. , E. Lindahl, GROMACS 4: algorithm for highly efficient, load-balanced, and scalable molecular simulation, J. Chem. Theory Comput. 4 (2008) 435–447.
[31] A.W. Sousa da Silva, W.F. Vranken, ACPYPE — AnteChamber PYthon Parser interfacE, BMC res. notes 5 (2012) 367.
[32] T.E. Cheatham, J.L. Miller, T. Fox, T.A. Darden, P.A. Kollman, Molecular-dynamics simulations on solvated biomolecular systems — the particle mesh Ewald method leads to stable trajectories of DNA, RNA, and proteins, J. Am. Chem. Soc. 117 (1995) 4193–4194.
[33] J.P. Ryckaert, G. Ciccotti, H.J.C. Berendsen, Numerical integration of the Cartesian equations of motion of a system with constraints: molecular dynamics of n-alkanes, J. Comput. Phys. 23 (1977) 327–341.
[34] H.J.C. Berendsen, J.P.M. Pstma, W.F. van Gusteren, A. Di Nola, J.R. Haak, Molecular dynamics with coupling to an external bath, J. Comput. Phys. 81 (1984) 3684–3690.

[35] M. Parrinello, A. Rahman, Polymorphic transitions in single-crystals — a new molecular-dynamics method, J. Appl. Phys. (1981) 7182–7190.
[36] W. Humphrey, A. Dalke, K. Schulten, VMD: visual molecular dynamics, J. Mol. Graph. 14 (1996) 33–38(27–38).
[37] M.A. Bjornsti, A.M. Knab, P. Benedetti, Yeast *Saccharomyces cerevisiae* as a model system to study the cytotoxic activity of the antitumor drug camptothecin, Cancer Chemother. Pharmacol. 34 Suppl. (1994) S1–S5.
[38] N. Kim, S.N. Huang, J.S. Williams, Y.C. Li, A.B. Clark, J.E. Cho, T.A. Kunkel, Y. Pommier, S. Jinks-Robertson, Mutagenic processing of ribonucleotides in DNA by yeast topoisomerase I, Science 332 (2011) 1561–1564.
[39] H. Interthal, P.M. Quigley, W.G. Hol, J.J. Champoux, The role of lysine 532 in the catalytic mechanism of human topoisomerase I, J. Biol. Chem. 279 (2004) 2984–2992.
[40] A. Tanizawa, R. Beitrand, G. Kohlhagen, A. Tabuchi, J. Jenkins, Y. Pommier, Cloning of Chinese hamster DNA topoisomerase I cDNA and identification of a single point mutation responsible for camptothecin resistance, J. Biol. Chem. 268 (1993) 25463–25468.
[41] X.G. Li, P. Haluska Jr., Y.H. Hsiang, A.K. Bharti, D.W. Kufe, L.F. Liu, E.H. Rubin, Involvement of amino acids 361 to 364 of human topoisomerase I in camptothecin resistance and enzyme catalysis, Biochem. Pharmacol. 53 (1997) 1019–1027.
[42] J.E. Chrencik, B.L. Staker, A.B. Burgin, P. Pourquier, Y. Pommier, L. Stewart, M.R. Redinbo, Mechanisms of camptothecin resistance by human topoisomerase I mutations, J. Mol. Biol. 339 (2004) 773–784.
[43] A. Coletta, A. Desideri, Role of the protein in the DNA sequence specificity of the cleavage site stabilized by the camptothecin topoisomerase IB inhibitor: a metadynamics study, Nucleic Acids Res. (2013).
[44] C. Tesauro, B. Morozzo Della Rocca, A. Ottaviani, A. Coletta, L. Zuccaro, B. Arno, I. D'Annessa, P. Fiorani, A. Desideri, Molecular mechanism of the camptothecin resistance of Glu710Gly topoisomerase IB mutant analyzed in vitro and in silico, Mol. Cancer 12 (2013) 100.
[45] B. Arnò, I. D'Annessa, C. Tesauro, L. Zuccaro, A. Ottaviani, B. Knudsen, P. Fiorani, A. Desideri1, Replacement of the human topoisomerase linker domain with the plasmodial counterpart renders the enzyme camptothecin resistant, PLoS One 8 (2013) e68404.